Developmental Biology 319 (2008) 346–358

Contents lists available at ScienceDirect

Developmental Biology

journal homepage: www.elsevier.com/developmentalbiology

Wise promotes coalescence of cells of neural crest and placode origins in the trigeminal region during head development

Yasuyo Shigetani [a], Sara Howard [a,1], Sonia Guidato [a,1], Kenryo Furushima [b], Takaya Abe [b], Nobue Itasaki [a,*]

[a] Division of Developmental Neurobiology, MRC National Institute for Medical Research, The Ridgeway, Mill Hill, London NW7 1AA, UK
[b] Laboratory for Animal Resources and Genetic Engineering, Center for Developmental Biology (CDB), RIKEN Kobe, 2-2-3 Minatojima Minamimachi, Chuo-ku, Kobe 650-0046, Japan

ARTICLE INFO

Article history:
Received for publication 1 December 2007
Received 24 April 2008
Accepted 25 April 2008
Available online 7 May 2008

Keywords:
Wnt signaling
Wise
Chick
Mouse
Trigeminal region
Neural crest cells
Placodal cells
Wnt6

ABSTRACT

While most cranial ganglia contain neurons of either neural crest or placodal origin, neurons of the trigeminal ganglion derive from both populations. The Wnt signaling pathway is known to be required for the development of neural crest cells and for trigeminal ganglion formation, however, migrating neural crest cells do not express any known Wnt ligands. Here we demonstrate that Wise, a Wnt modulator expressed in the surface ectoderm overlying the trigeminal ganglion, play a role in promoting the assembly of placodal and neural crest cells. When overexpressed in chick, Wise causes delamination of ectodermal cells and attracts migrating neural crest cells. Overexpression of Wise is thus sufficient to ectopically induce ganglion-like structures consisting of both origins. The function of Wise is likely synergized with *Wnt6*, expressed in an overlapping manner with *Wise* in the surface ectoderm. Electroporation of morpholino antisense oligonucleotides against *Wise* and *Wnt6* causes decrease in the contact of neural crest cells with the delaminated placode-derived cells. In addition, targeted deletion of *Wise* in mouse causes phenotypes that can be explained by a decrease in the contribution of neural crest cells to the ophthalmic lobe of the trigeminal ganglion. These data suggest that Wise is able to function cell non-autonomously on neural crest cells and promote trigeminal ganglion formation.

Introduction

The trigeminal nerve is the largest cranial nerve, containing both sensory and motor neurons responsible primarily for sensation in the face and movement for mastication. The trigeminal ganglion consists of two lobes, the ophthalmic and maxillomandibular lobes, the latter of which further bifurcates to upper and lower jaws. The ganglion comprises cells which derive from three distinct origins: two different ectodermal placodes – the ophthalmic trigeminal (opV) and maxillomandibular trigeminal (mmV) placodes – which contribute cutaneous sensory neurons to the distal regions of their respective ganglionic lobes and; the neural crest, which contributes cutaneous and some proprioceptive neurons to the proximal region of the ganglion, as well as all satellite glial cells (D'Amico-Martel and Noden, 1983; Hamburger, 1961). Placodal cells delaminate from the ectodermal layer and migrate into the mesenchymal space, where they meet neural crest cells that have migrated from the dorsal neural tube.

Importance of the coalescence of the neural crest and placodal populations for trigeminal ganglion formation has been shown by experimental removal of each of the populations in the chick embryo (Hamburger, 1961; Moody and Heaton, 1983b; Stark et al., 1997). Removal of neural crest cells results in ganglia positioned deep under the ectoderm in which the ophthalmic and maxillomandibular lobes have become separated, and there is a lack or a delay in the formation of their connections with the hindbrain (Hamburger, 1961; Moody and Heaton, 1983b; Stark et al., 1997). This suggests that while neural crest cells are not required for the delamination and migration of placodal cells, they serve as an aggregation centre for the fusion of the two placode-derived cell populations, and assist in the formation of the neuronal connection between the ganglion and hindbrain. Ablation of placodal cells, on the other hand, although difficult to achieve completely because of placode regeneration, results in the formation of trigeminal ganglia in normal positions and with connections to the hindbrain, but of variable sizes and with peripheral projection defects (Hamburger, 1961). These defects, including absence of ophthalmic and/or maxillary branches, suggest that placodal cells function as pioneers for axonal path-finding and projections (Baker and Bronner-Fraser, 2001; Hamburger, 1961; Moody and Heaton, 1983a; Moody and Heaton, 1983b). Thus, both the neural crest population and the placodal population have distinct roles to play in the formation of the trigeminal ganglion. Supporting their instructive role in the assembly of the two populations, trigeminal placodal cells have a strong tendency to coalesce with neural crest cells; even in ectopic locations at the trunk level, neurons derived from grafted ophthalmic placode contribute to dorsal root ganglia, which are normally formed solely by neural crest-derived cells (Baker et al., 2002).

* Corresponding author.
E-mail address: nitasak@nimr.mrc.ac.uk (N. Itasaki).
[1] These authors contributed equally to this work.

0012-1606/$ – see front matter.
doi:10.1016/j.ydbio.2008.04.033

The Wnt signaling pathway is involved in multiple steps of the development of neural crest cells, with both the Wnt/β-catenin and Wnt/planar cell polarity (PCP) pathways being implicated in these processes. For example, while Wnt/β-catenin is involved in the specification, proliferation and fate determination of neural crest cells (Brault et al., 2001; Burstyn-Cohen et al., 2004; De Calisto et al., 2005; García-Castro et al., 2002; Hari et al., 2002; Ikeya et al., 1997; Lewis et al., 2004; Saint-Jeannet et al., 1997; Taneyhill and Bronner-Fraser, 2005), the Wnt/PCP pathway is required for their migration (De Calisto et al., 2005). Little is currently known about the molecular mechanisms underlying the induction of the trigeminal placodes, although it has been recently shown that opV placode cells require the Wnt/β-catenin pathway in order to adopt or maintain an opV fate (Lassiter et al., 2007).

Despite the repeated requirement of Wnt pathway activation during their development, neural crest cells do not express Wnt ligands after migrating out of the dorsal neural tube. The lack of any known Wnt mRNA expressed in the migrating neural crest cells suggests that the ligand may be provided cell non-autonomously by other tissues. Wise is a secreted Wnt signal modulator expressed in many regions including ectodermal derivatives. In the cranial region of 3-day chick embryos, *Wise* is expressed strongly in the surface ectoderm of the trigeminal region, including the periocular region, the maxillary prominence and the mandibular arch (Shigetani and Itasaki, 2007). Wise functions in multiple ways: by binding to LRP6, Wise either enhances or inhibits the function of Wnt ligands depending on the partner Wnt ligand (Beaudoin et al., 2005; Guidato and Itasaki, 2007; Yanagita et al., 2004). Wise is also able to affect the Wnt/PCP pathway (Itasaki et al., 2003), possibly by interacting with LRP6, which has also been suggested to be involved in the pathway (Tahinci et al., 2007). As Wise alone does not activate Wnt receptors (Guidato and Itasaki, 2007), exerting its function requires an accompanying Wnt ligand. A candidate for the Wise partner in the chick cranial region is Wnt6, which is co-expressed with Wise in the head ectoderm on the trajectories of the trigeminal nerves at ganglionic stages (Schubert et al., 2002). In this study we demonstrate that Wise promotes coalescence of neural crest cells and placodal cells to form ganglion-like structures. This is likely to be achieved by delamination of ectodermal cells and the attraction of neural crest cells to them. Loss of function analyses in chick and mouse support the idea that the coalescence of neural crest cells to the placode-derived cells may have been decreased when Wise expression is compromised. These data suggest that Wise is able to function cell non-autonomously on neural crest cells and promote trigeminal ganglion formation.

Materials and methods

Virus infection

Chick *Wise* cDNA (Itasaki et al., 2003) was subcloned into RCAS(A) vector (Petropoulos and Hughes, 1991). As a control, human placental alkaline phosphatase (ALP) in the RCAS(A) vector (Fekete and Cepko, 1993) was used. Retrovirus was made as described previously (Itasaki and Nakamura, 1996). Viral solution was injected into the neural canal and the space underneath the vitelline membrane of SPF chick embryos (Institute for Animal Health, England) at Hamburger and Hamilton (HH) stages 8 to 9 (Hamburger and Hamilton, 1951), and the embryos were incubated for up to two days before harvesting.

Chick electroporation

In ovo electroporation in chick embryos was performed at HH stages 9 to 10 as described previously (Itasaki et al., 1999). For electroporation in the neural crest, plasmid DNA was injected into the lumen of the neural tube and electrodes were positioned bilaterally. For electroporating into the surface ectoderm, DNA was injected in the space between the vitelline membrane and the embryo, and the cathode was placed on the vitelline membrane while the anode was in the yolk beneath the endoderm. Chick *Wise* cDNA was subcloned into pCAGGS (Momose et al., 1999) with IRES-GFP. To make a *Wnt6* expression construct in the same vector, a chick EST clone was obtained from GeneService (899f16). Since this clone misses the first 9 amino acid coding region (a part of the signal sequence), the signal sequence of mouse *Kremen2*, combined to a myc tag, was attached to the signal sequence cleavage site of chick *Wnt6*, as predicted from mouse *Wnt6*. The expression of electroporated genes was monitored by the GFP expression and detected by anti-GFP antibody (Molecular Probes).

Embryo staining

In situ hybridization and immunostaining were performed following standard protocol (Ogasawara et al., 2000). Antibodies used are: HNK1 (BD Biosciences); anti-neurofilament-associated protein antibody, 3A10 (DSHB); anti-GFP antibody (Molecular Probes); anti-viral gag antibody, 3C2 (DSHB); anti-Islet-1/2 antibody, 4D5 (DSHB). For the staining of actin filaments, phalloidin-FITC (Sigma) was used. For double staining of *in situ* hybridization and immunostaining, embryos were first processed for *in situ* hybridization detecting digoxigenin labeled probes for *Pax3* or *Brn3a* with anti-digoxigenin alkaline phosphatase with NBT and BCIP (purple), followed by incubation with HNK1 antibody, which was detected by HRP conjugated secondary antibody and diaminobenzidine (brown), or using anti-GFP-antibody and FITC-conjugated secondary antibody. When required, embryos were cryosectioned at 12 μm before immunostaining.

Cell lineage analyses

For cell lineage analyses (Figs. 2E,F), embryos were electroporated with *GFP* in the neural tube at stages between HH 9$^-$ and 10 and infected with *Wise* virus. Once the neural tube had become closed, requiring 3–8 h of incubation, the head ectoderm was labeled by injecting DiI solution into the space between the vitelline membrane and the embryo (Stark et al., 1997). Embryos were incubated for a further 1.5 days and analyzed under an epifluorescent microscope.

Implantation of cell aggregates

For quantitative analyses of neural crest cell migration into fibroblast cell aggregates (Figs. 3A–G), chick fibroblasts infected with virus encoding either *ALP* or *Wise* were aggregated *in vitro* by a hanging-drop in DMEM. Aggregates were labeled with CellTracker (Molecular Probes) in red and grafted into embryos that had been electroporated with GFP in the neural fold. The aggregates were positioned adjacent to the midbrain underneath the surface ectoderm at HH stages 9$^-$ to 9$^+$. Embryos were cultured until they reached HH stage 11. Embryos from each group with comparable aggregate size and comparable expression of GFP in the neural tube were processed for cryosectioning. In each embryo, serial transverse sections were made at 12 μm thickness. Typically, the grafted cell aggregates were spanned in 9 serial sections, among which the section containing the largest number of neural crest cells was used for quantification. The number of GFP-positive neural crest cells in the aggregate was counted. The area of the cell aggregate was also measured. Cases where largest surface area of the aggregate was less than 1000 μm^2 were excluded from the analysis. If the neural crest cells were on the edge of the aggregate, only the cells that were surrounded by the aggregate cells by more than half of the edge were counted. The number of neural crest cells in each case was normalized to the average surface area of the cell aggregate for comparison (See Supplementary Table 1).

In vitro culture of neural crest cells

To examine the effect of Wise on neural crest cell morphology (Figs. 3H–R), the midbrain was explanted from HH stages 8$^+$ to 9 embryos on coverslips that had been coated with a sheet of chick fibroblast cells expressing either *ALP* or *Wise*. The explant was covered with thin collagen and cultured for two days before processing for staining with either 3C2 antibody (Figs. 3I,K) or phalloidin-FITC (Figs. 3M,N,P,Q) and with HNK1 antibody. The longest stretch of HNK1-positive cells was measured using confocal microscopy for 56 cells in each group, from 6 independent explants. Fig. 3R shows the average length and the standard deviation.

Electroporation of morpholino antisense oligonucleotides

Morpholino oligonucleotides against chick *Wnt6* (5′-TGAGGCCGGACCTTAC**CCTG-CTGCA**-3′, spanning the boundary between the second exon and the second intron; bold is the end of the second exon) and *Wise* (5′-GAATGGCGGAGAGAAG**CAT**GATTGG-3′, beginning of the coding; bold indicates the complementary sequence to the first methionine codon) were custom-made and conjugated with Fluorescein (Gene Tools). A 1:1 mix of these morpholinos were used at the concentration of 100 μM dissolved in H_2O. For a control, a standard control morpholino oligo conjugated with fluorescein provided by the supplier was used. Based on a weak positive charge of fluorescein and no charge of morpholino oligonucleotides, the morpholino was electroporated on the surface ectoderm by placing the anode on the dorsal side of embryos and the cathode on the ventral side. Embryos were incubated until HH stages 14 to 15, and only the embryos showing green fluorescence in the trigeminal region were harvested. Embryos were stained for *Brn3a* and HNK1 in whole mounts, followed by cryosectioning. The inhibitory effect of morpholinos was evaluated either by RT-PCR of electroporated embryos with *Wnt6* splice blocking morpholino, or by *in vitro* translation for *Wise* translation initiation blocking morpholino (Supplementary Fig. 4).

Targeted deletion of Wise in mouse

The *Wise* mutant mice (Accession number: CDB0048K) were generated with TT2 embryonic stem cells as described (Murata et al., 2004; Yagi et al., 1993). *Wise* genomic

fragments were isolated from a C57BL/6 BAC clone and inserted into a DT-A/AFP/Neo cassette (http://www.cdb.riken.go.jp/arg/cassette.html) so that the first exon following the translation initiation codon was replaced with AFP (Supplementary Fig. 6).

Results

Wise induces ectopic ganglia in the trigeminal region

In the developing chick embryo head at HH stage 20, *Wise* is expressed in the surface ectoderm, particularly strongly in the ectoderm overlying the trajectory of the ophthalmic nerve, the dorsal edge of the eye, the maxillary prominence and the mandibular arch (Shigetani and Itasaki, 2007). *Wise* expression in the cranial region begins, although faintly, at HH stage 11 at the midbrain level (Supplementary Fig. 1). This is substantially later than the commitment of ectodermal cells to adopt the placodal fate or the start of *Pax3* expression in the opV placode at HH stage 8 (Stark et al., 1997). The initiation of *Wise* expression at HH stage 11 coincides with the timing of initial delamination of opV placodal cells encountering migrating neural crest cells (Stark et al., 1997). To investigate Wise function in the cranial region, *Wise* was overexpressed in the head region by retroviral infection at HH stages 9⁻ to 10 and analyzed at HH stages 18 to 22. The control ALP virus-infected embryos did not show any significant phenotypes in the pattern of HNK1 staining (n=33, of which 29 were stained with *ALP* and HNK1, and 4 were stained with *Pax3* and HNK1) (Figs. 1A,C). In contrast, striking phenotypes were observed after *Wise* virus infection (Figs. 1B,D–K) (n=71/95; out of 95, 5 were stained with HNK1 only, 55 were stained with *Wise* and HNK1, 25 were stained with *Pax3* and HNK1, and 10 were stained with *Wise* and 3A10). Ectopic ganglia of various sizes were induced adjacent to the midbrain and isthmus, from two pairs of large ganglia (Fig. 1B) to micro-ganglion-like structures (Fig. 1E). The majority of the embryos showed ectopic ganglia adjacent to the isthmus (n=47/71, of which 25 had ectopic ganglia on both right and left sides), while others showed ones anteriorly near the diencephalon-midbrain junction (n=12/71, of which 5 had ectopic ganglia on both sides) or at both anterior and posterior sides of the midbrain (n=12/71, of which 2 had ectopic ganglia only on one side). Ectopic ganglia often extended axons which either followed the trajectory of the ophthalmic nerves from the trigeminal ganglion proper or, at a lesser frequency, connected to the facial-acoustic ganglia (the embryo shown in Fig. 1B exhibits both cases in two different ectopic ganglia). We found that some ectopic ganglia are positive for *Pax3* (Fig. 1F), which is normally expressed strongly in opV placode-derived cells and at a lower level in neural crest-derived glial cells in sensory ganglia (Baker et al., 2002; Goulding et al., 1991; Stark et al., 1997), suggesting that those ectopic ganglia exhibit the phenotype of sensory ganglia. As some of the ectopic ganglia became visible only after the HNK1 staining (22 out of 25 embryos showed ectopic ganglia after HNK1 staining), we were unable to accurately judge how many of the ectopic ganglia were *Pax3*-positive. Staining with *Wise* showed ganglion-like structures (Fig. 1G), and double staining with HNK1 further revealed assemblies of HNK1-positive cells, without clear axonal extension, containing *Wise*-positive cells (n=40/55) (Fig. 1H). The HNK1-positive cell assemblies consisted of both *Wise*-positive and *Wise*-negative cells (Fig. 1I). In addition, ectopic ganglia contained neurofilament, indicative of neuronal differentiation (Figs. 1J,K). These results suggest that ectopically expressed Wise is capable of inducing cell assemblies, some of which show ganglion-like structures with axons, likely by functioning in both cell autonomous and non-autonomous manners.

It was noted that about 15% of analyzed embryos showed slightly deformed brain structures, both in the control virus and *Wise* virus injected embryos. This is likely due to the dorsal midbrain becoming stuck to the vitelline membrane, which generally occurs after *in ovo* manipulation. In addition, some embryos infected with *Wise* virus seemed to develop a smaller midbrain compared to control embryos (Figs. 1B,E, for example). We found that overexpression of *Wise* in the neural tube attenuated *en1* expression (Supplementary Fig. 2), which could be, at least in part, a cause of the under-developed midbrain. Since loss-of-function mutation of *en1* does not affect trigeminal ganglion formation (Wurst et al., 1994), we considered that that the phenotype of ectopic ganglia obtained by *Wise* virus infection is not due to the defects in midbrain formation, hence the trigeminal nerve formation was further analyzed.

To determine whether it is the neural crest cells, the surface ectoderm cells or both that are responsible for the ectopic ganglia, these tissues were electroporated separately with *Wise*. Overexpression of *Wise* in the neural crest did not cause any obvious effect on the cranial nerve patterns revealed by HNK1 (n=0/30, data not shown). In contrast, *Wise* electroporation on the surface ectoderm recapitulated the effect of virus infection and induced ectopic ganglia as revealed by *Pax3* expression (n=8/24, Fig. 2B). Electroporation of GFP plasmid did not show any effect (n=0/13, Fig. 2A). It was noted that *Wise* virus infection caused more significant phenotypes compared to electroporation in the surface ectoderm, both in the frequency of positive cases and in the number of ectopic ganglia noticeable by whole mount analyses. One possible reason is that virus infection can cause overexpression of Wise both in the neural crest cells and surface ectoderm, which may facilitate initiating the ganglion-like formation.

In vitro studies have shown that Wise enhances or inhibits the function of Wnt ligands (Guidato and Itasaki, 2007). Since *Wnt6* is expressed in an overlapping manner with *Wise* in the cranial surface ectoderm at the ganglionic stage (Schubert et al., 2002), we tested whether ectopic *Wnt6* also affects ganglion formation. Electroporation of *Wnt6* into the surface ectoderm induced ectopic ganglia in a similar manner to *Wise* (n=14/30, Fig. 2C). Co-electroporation of *Wise* and *Wnt6* showed a similar effect to each alone (n=16/30, Fig. 2D), suggesting that Wise in the context of ganglion formation synergizes with *Wnt6*, rather than inhibiting it. In the overexpression experiment, the synergistic effect was not significant, presumably because the overexpression of each is sufficient to cause a saturated degree of pathway activation.

The composition of ectopic ganglia induced by Wise was examined by labeling cells of neural crest and surface ectoderm

Fig. 1. Induction of ectopic ganglia by *Wise* retroviral infection. (A,B) Control (A) and *Wise*-virus-infected (B) embryos at HH stages 21–22 stained with HNK1 antibody revealing axonal patterns. (C,D) Camera lucida drawings of embryos shown in panels A,B. tel, telencephalon; di, diencephalon; mes, mesencephalon; rh, rhombencephalon; e, eye; mx, maxillary process; md, mandibular process; ot, otic vesicle; V, trigeminal ganglion; opV, ophthalmic branch of the trigeminal ganglion; mmV, maxillomandibular branch of the trigeminal ganglion; VII+VIII, facial-acoustic ganglia; IX, petrosal ganglion; X, nodose ganglion; XII, hypoglossal nerves; GR1 and GR2, Ectopic ganglion 1 and 2 on the right side; GL1 and GL2, Ectopic ganglion 1 and 2 on the left side. The ectopic ganglion GL1 has a connection to the ophthalmic branch of the trigeminal ganglion. GL2 is connected to the facial-acoustic ganglion. (E–K) *Wise*-virus-infected embryos with ectopic micro-ganglia-like structures (arrows) at HH stages 18–19 stained with HNK1 antibody (E), for *Pax3* (F), for *Wise* (G), for both *Wise* and HNK1 (H,I) and for *Wise* and neurofilament (NF) (J,K). Panel E shows small ectopic ganglia adjacent to the diencephalon and anterior and posterior midbrain (arrows). All ectopic ganglia are connected to the ophthalmic nerve in this case. The trigeminal ganglion (V) is deformed, which might be due to the under-developed midbrain causing deformity in the isthmus region. Panel F is a magnified lateral view of the trigeminal region showing a *Pax3*-positive ectopic ganglion (arrow) connected to the ophthalmic ganglion (opV). The maxillomandibular ganglion (mmV) is weakly positive for *Pax3*. m, midbrain; h, hindbrain. Panel G is a dorsal view of the midbrain stained with *Wise* after virus infection. In addition to the speckled pattern of staining (small dots), ectopic ganglion-like structures are seen (arrows). (H) A lateral view of an embryo co-stained for *Wise* (purple) and with HNK1 (brown) revealing that small assemblies of HNK1-positive cells (brown) are seen adjacent to the isthmus, in addition to the large endogenous ophthalmic (opV) and maxillomandibular (mmV) ganglia. A high magnification in panel I shows that the assemblies contain *Wise*-positive cells (purple, arrows); however, not all cells are *Wise*-positive. Panel J shows an embryo co-stained with *Wise* and 3A10 detecting neurofilament (NF). A *Wise*-positive micro-ganglion is seen near the anterior midbrain (arrow). Panel K is a transverse section of a similar embryo showing a *Wise*-positive ectopic ganglion-like structure (purple) on the surface of the midbrain. Neurofilament (brown) is seen in the ganglion-like structure as indicated by arrow. Arrowheads show endogenously developing neurofilaments in the midbrain.

separately. At the same time as the *Wise* virus injection at stages HH 9⁻ to 10, neural crest cells were labeled by electroporating *GFP* DNA into the open neural fold, and embryos were incubated for 3–8 h until the neural tube closed completely. The surface ectoderm was then labeled with DiI and the embryos were incubated for a further two days. Among 13 embryos, two showed clear ectopic ganglia labeled with both GFP and DiI (Fig. 2E,F), suggesting that ectopic ganglia consist of cells of both origins. There was no case of ectopic ganglia with single labeling.

Wise promotes delamination of surface ectoderm cells

The induction of ectopic ganglia was studied at younger embryos at HH stage 13 on sections. Embryos were electroporated on the surface ectoderm with control vector or *Wise*. Judged by the IRES-GFP expression derived from the expression vector, embryos with ectopic ganglia (Wise, $n=8$) were chosen to process together with control-electroporated embryos ($n=8$) for cryosections and stained with HNK1 to reveal migrating neural crest cells at this stage. In the

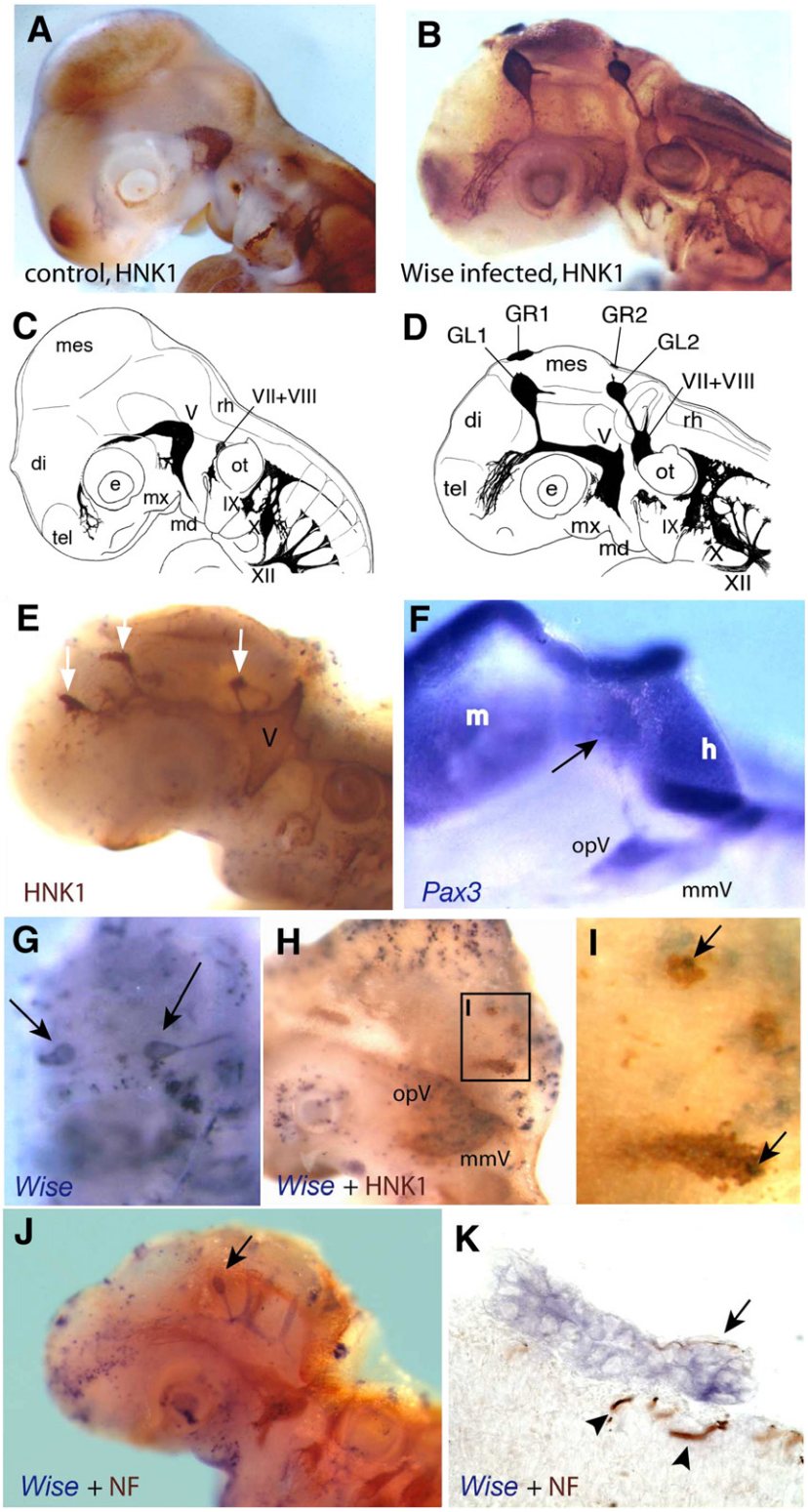

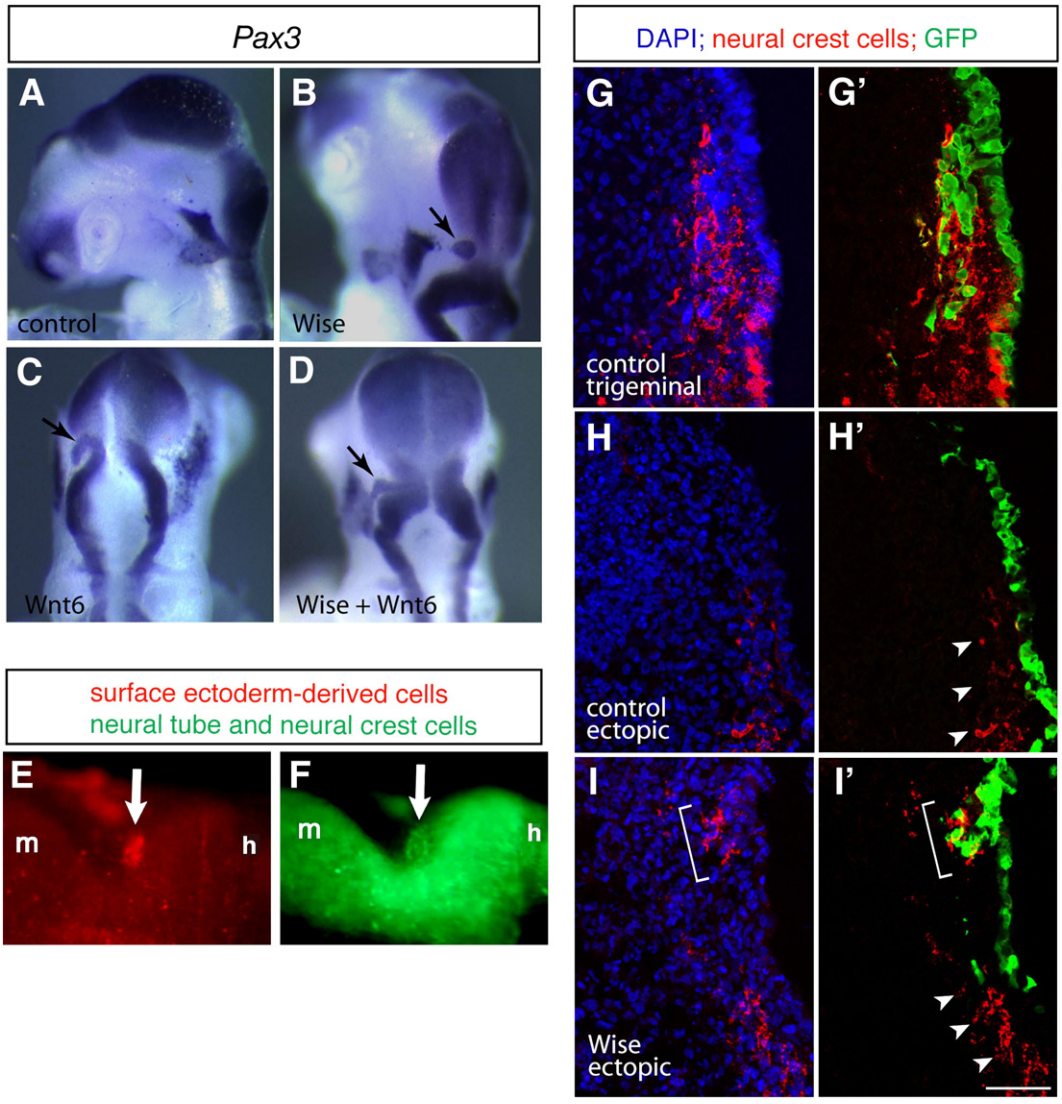

Fig. 2. The effect of overexpression of Wise and Wnt6 in the trigeminal region. (A–D) Embryos electroporated on the surface ectoderm at HH stages 9–10 with constructs of GFP (control, A), *Wise* (B), *Wnt6* (C) or *Wise*+*Wnt6* (D), harvested at HH stages 18–20 and stained for *Pax3*. (A), lateral view; (B), dorsal–lateral view; (C) and (D), dorsal view. Arrows indicate ectopically induced *Pax3*-positive ganglion-like structures. (E,F) A lateral view of a whole-mount embryo at HH stage 16 with an ectopic ganglion (arrow) after *Wise* virus infection. The neural tube and neural crest cells were labeled with GFP (green, F) by electroporation at HH stages 9⁻ to 10 at the time of virus injection, while the derivatives of the surface ectoderm were labeled with DiI (red, E) after neural tube closure. The induced ectopic ganglion (arrow) is positive for both origins. m, posterior midbrain; h, anterior hindbrain. (G–I) Transverse sections of HH stage 13 embryos electroporated on the surface ectoderm at HH stages 9–10 with control (G,H) or *Wise* (I) construct in an IRES-GFP vector. Dorsal is to the top. Electroporated cells are revealed in green (detected by anti-GFP antibody) while neural crest cells are shown in red (revealed by HNK1 antibody). Nuclei are stained with DAPI (blue). Panel G shows the level of the trigeminal region in the control-electroporated embryo. Many migrating neural crest cells are found to intermingle with delaminated ectoderm-derived cells. Panels H and I show a region at the anterior midbrain level. While the control embryo (H) does not show any significant delamination of electroporated cells, the *Wise*-electroporated embryo (I) shows delamination of surface ectoderm, which forms a cluster and is surrounded by neural crest cells (bracket). In both panels H and I, a stream of neural crest cells migrating further ventrally are seen (arrowheads in panels H′ and I′). Scale bar, 50 μm.

trigeminal region of all cases, cells delaminated from the placode were found to be intermingled with neural crest cells (Fig. 2G and data not shown). In embryos electroporated with *Wise*, additional clusters of delaminated cells were seen in ectopic regions adjacent to the anterior midbrain (Fig. 2I). This showed that Wise was able to ectopically induce delamination of surface ectoderm cells. It appeared that the delaminated cluster was gathered with neural crest cells; however, it was difficult to analyze in a quantitative manner whether there was any significance in the attraction of neural crest cells to the ectopically delaminated cluster or not, since the region is on the normal path of neural crest cells. Regardless of ectopic delamination, the majority of the neural crest cells migrate underneath the ectoderm without contributing to ganglion formation (Fig. 2H). Hence a question remained as to whether or not delaminated cells form ectopic ganglia by positively attracting and integrating neural crest cells.

Wise attracts neural crest cells

The result that ectopically delaminated ectodermal cells after Wise electroporation are surrounded by neural crest cells (Fig. 2I) led us to study whether the Wise-induced delaminated ectodermal cells instructively attract neural crest cells or not. To test this, aggregates of chick fibroblasts expressing either control ALP or Wise were implanted on the route on which neural crest cells migrate. It was found that neural crest cells enter the Wise-expressing cell aggregates more frequently compared to control ALP-expressing ones (Figs. 3A–G, Supplementary Table 1). It was also noted that neural crest cells in the Wise-expressing cell aggregates extend sharp processes more than the ones in control aggregates. To further analyze process extension in the neural crest cells, they were cultured *in vitro* with control (*ALP*)- or *Wise*-expressing fibroblast cells (Figs. 3H–Q) and the length of the neural crest cells were quantified. In the presence of Wise, neural crest

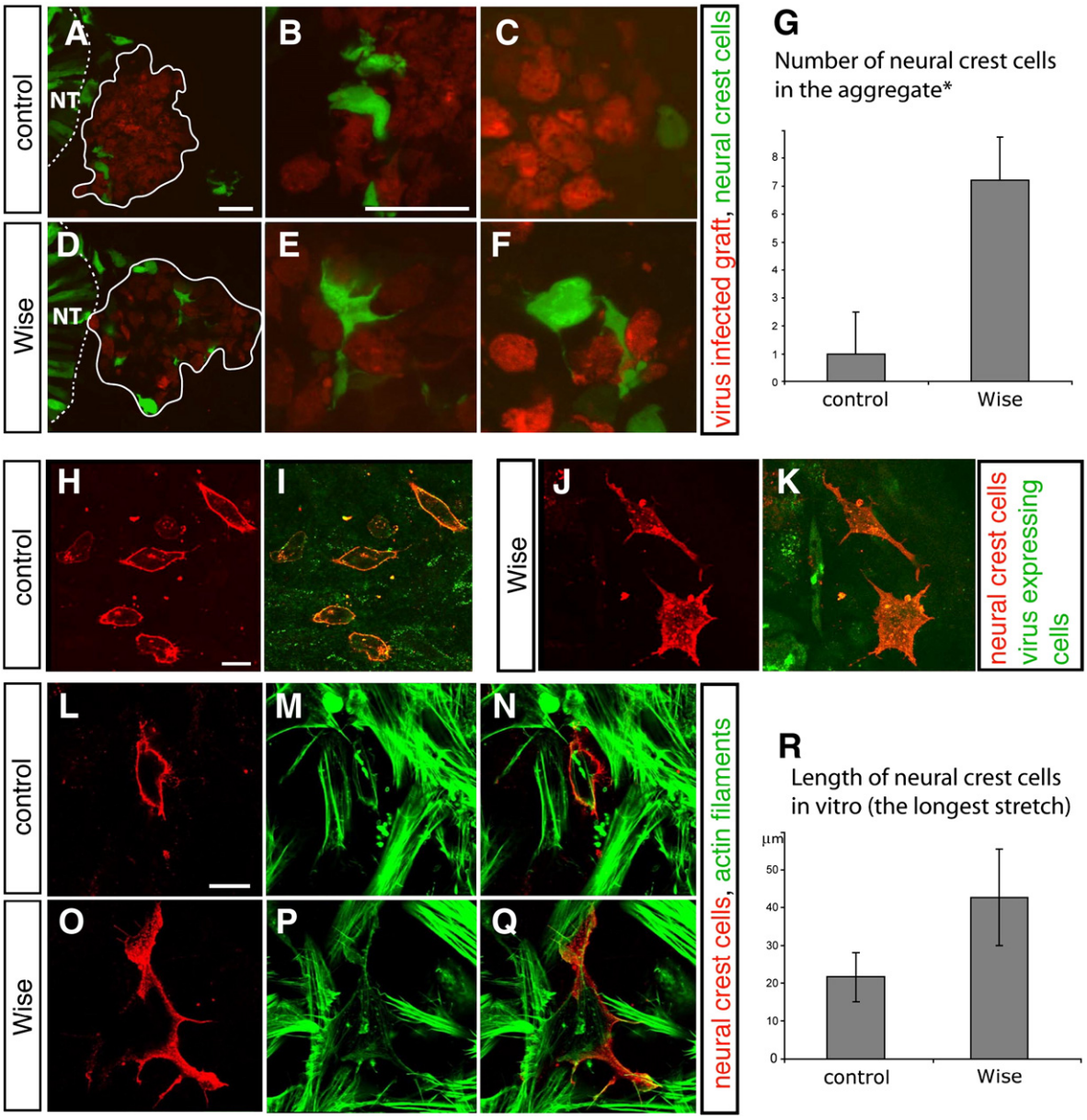

Fig. 3. Neural crest cells are attracted to Wise-expressing fibroblasts *in vivo* and extend long processes *in vitro*. (A–F) Sections of HH stage 11 embryos in which aggregates of fibroblasts infected with either *ALP* (control, A–C) or *Wise* (D–F) encoding virus had been implanted next to the midbrain at HH stages 8$^+$ to 9. The cell aggregates, outlined in panels A and D, had been labeled with CellTracker™ in red. In both cases, the neural tube (NT) was electroporated with *GFP* before the cell aggregate was grafted, in order to trace the neural crest cells (green). Compared to the control (A), Wise-expressing cell aggregate shows many neural crest cells inside of the aggregate (D). Panels B and E are higher magnifications of panels A and D, respectively. Panels C and F are sections of different embryos from panels A and D, in the same magnification as panels B and E. In the case of panel C, there was no neural crest cell in the aggregate; only one was found adjacent to the aggregate. Scale bars, 20 μm. (G) Quantitative analysis of neural crest cells incorporated into the fibroblast cell aggregate. The *Y* axis shows the number of neural crest cells found in the fibroblast aggregate on a section which contained the maximum number of neural crest cells in the aggregate, normalized by the average surface area of the cell aggregate (*See Supplementary Table 1 for details of quantification). Four embryos for each group were analyzed. In control, two out of four embryos showed no neural crest cells in the aggregate. Figs. 3A–B present the cases that had neural crest cells in the aggregate. Wise-expressing cell aggregates comprise more neural crest cells compared to ALP-expressing aggregates. Student's *t*-test; $p<0.02$. (H-Q) *In vitro* culture of neural crest cells from the midbrain, co-cultured with chick fibroblasts infected with either *ALP* (H,I, L-N) or *Wise* (J,K,O-Q) virus. Neural crest cells, recognized by HNK1 antibody, are shown in red. In panels I and K, the virus expressing cells are stained with 3C2 antibody in green. In panels M, N, P and Q, actin filament is stained in green. Neural crest cells cultured with Wise expressing cells are significantly stretched and show long processes compared to the ones cultured with ALP expressing cells. In panel P, the neural crest cell (red) shows stretched processes that attach to the Wise-expressing fibroblasts (HNK1-negative green cells). Scale bars, 10 μm. Panel R shows a quantitative analysis measuring the longest stretch of neural crest cells in each group. Fifty six cells were analyzed in each group from six independent explants. Student's t-test; $p<0.001$.

cells were more stretched and had long processes (Fig. 3R). These data show that neural crest cells respond to Wise cell non-autonomously, show affinity to Wise-expressing cells and stretch cellular processes, suggesting that Wise-expressing cells delaminated from the ectoderm may attract neural crest cells thus facilitating ganglion formation.

It was noted that Wise virus infection not only induces ectopic ganglia but also affects the position of the endogenous trigeminal ganglion and the nerve patterns. Among embryos without ectopic ganglia (n=24/95), thirteen showed abnormal nerve patterns or dislocation of the trigeminal ganglion (data not shown; similar phenotypes are seen in trigeminal nerves in Figs. 1B,F). To examine the relationship between nerve patterns and Wise expression, embryos were electroporated with control or *Wise* on the surface ectoderm and analyzed at HH stages 18 to 19 (n=8 for control, 10 for *Wise*). It was found that *Wise* electroporation on the surface ectoderm caused the location of trigeminal nerves to overlap with the *Wise*-electroporated

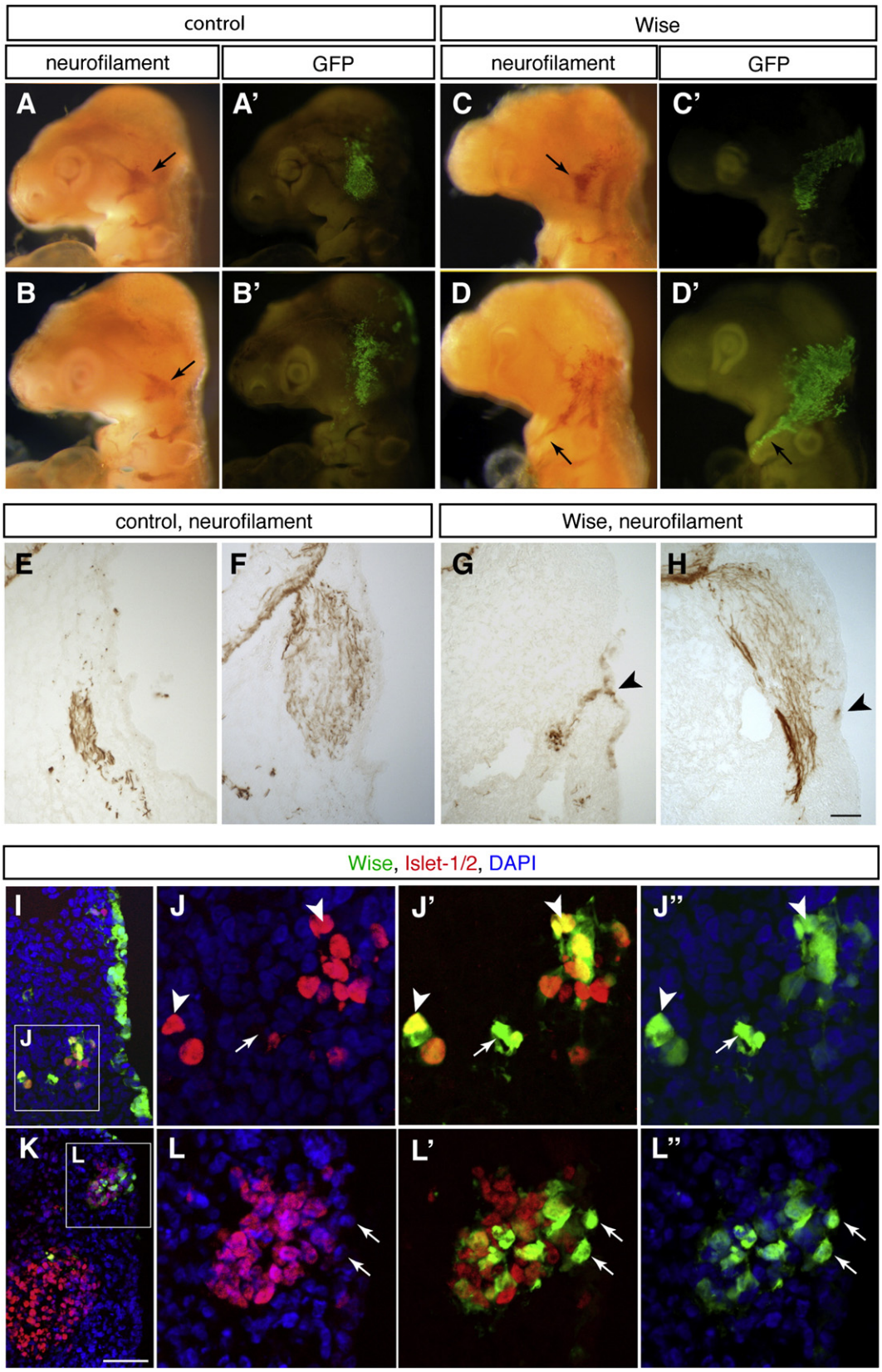

Fig. 4. Wise electroporation in the surface ectoderm biases trajectories of trigeminal nerves. (A–H) Embryos electroporated on the surface ectoderm with either control (A,B, E,F) or *Wise* (C,D, G,H) expression constructs with IRES-GFP at HH stages 9–10, harvested at HH stages 18–19 and stained for neurofilament and GFP. While control embryos show the normal trigeminal nerve patterns (A,B), *Wise*-electroporated embryos show abnormally restricted (C, arrow) or ectopically extended (D, arrow) trigeminal nerves, in an overlapping manner with the electroporated region (green in the dark field). Sections at the levels of ophthalmic branch (E,G) and maxillomandibular lobe (F, H) shows that Wise electroporation induces small populations of neurofilament-positive cells in the surface ectoderm (arrowheads in panels G,H. (I–L) Two different embryos electroporated on the surface ectoderm with *Wise* (green) and fixed at HH stages 18–19, showing ectopic assemblies of Wise-positive delaminated cells. Red shows Islet-1/2 staining indicative of sensory neurons. Nuclei are stained by DAPI (blue). Three different combinations of channels are shown (J–J″, L–L″). Arrows indicate Wise-positive, Islet-1/2-negative cells. Arrowheads show double positive cells for both Wise and Islet-1/2. Scale bars, 50 μm.

region, thereby deforming the endogenous trigeminal ganglion or inducing an ectopic projection (Figs. 4A–D). In one case a trajectory of nerves was ectopically found in the hyoid arch where trigeminal nerves do not normally innervate (Fig. 4D). In addition, histological analyses showed neurofilament-positive cells in the surface ectodermal layer in *Wise*-electroporated embryos (n=2/10; GFP control n=0/8) (Figs. 4E–H). These results suggest that *Wise* expression in the surface ectoderm may have a role not only in the assembly of trigeminal ganglion cells but also in the guidance of nerves underneath the ectoderm. To examine whether Wise misexpression induces neuronal cell fate, Wise-electroporated embryos were processed for cryosectioning and stained with Islet-1/2 which marks neurons in the trigeminal ganglion (Fedtsova et al., 2003) (n=9). We found that ectopically induced cell assemblies consisted predominantly of Islet-1/2-positive cells (Figs. 4I–L). However, a few of Wise-electroporated cells were Islet-1/2-negative (Figs. 4I-L), showing that Wise-overexpression does not sufficiently induce the neuronal fate. This suggests that Wise does not play an instructive role in neuronal differentiation.

The function of Wise was further investigated using a molecular marker for neurogenic placodal cells in embryos at HH stage 13. *Wise* electroporation on the surface ectoderm did not increase the number of or ectopically induce *Brn3a*-positive placode-derived sensory neuron precursors (Supplementary Fig. 3). Together with the fact that Wise is not expressed at the stage at which ectodermal cells adopt the placodal fate (HH stage 8) (Stark et al., 1997), it seems unlikely that Wise expressed on the surface ectoderm is involved in the fate determination of placodal cells. However, a possibility remains that ectodermal cells expressing exogenous Wise might have differentiated into sensory neurons without inducing *Brn3a*, since *Brn3a* is not a required factor for trigeminal ganglion formation in mice (McEvilly et al., 1996).

Loss-of-function analyses of Wise function

Attempts were made to investigate the endogenous roles of Wise and Wnt6, both of which are expressed in the surface ectoderm overlying the trigeminal region. Morpholino oligonucleotides against chick *Wise* and *Wnt6*, which attenuate the translation of each protein (Supplementary Fig. 4), were electroporated in the surface ectoderm at HH stages 9 to 10. Embryos were analyzed at HH stages 13 to 15 using HNK1 antibody, which reveals migrating neural crest cells at this stage, and *Brn3a*, which labels cells in the ophthalmic placode and delaminated neural progenitors contributing to the trigeminal ganglion (Begbie et al., 2002). During normal embryogenesis, cranial neural crest cells migrate out as a mass, first laterally then ventrally (Figs. 5A–C, brown). *Brn3a*-positive placodal cells appear in the surface ectoderm lateral to the mesencephalon at around HH stage 10 and increase rapidly at HH stages 11 to 12 (Figs. 5A–F, purple). The position of the *Brn3a*-positive cells shifts laterally as the embryo grows. Delamination of placodal cells starts at HH stage 11 and continues until HH stage 18 (Stark et al., 1997). The most medial part of the neural crest cell mass overlaps with the position of the *Brn3a*-positive placodal cells (Figs. 5B,C). This overlap becomes well-defined and is maintained as the embryo develops. In normal and control morpholino electroporated embryos (n=24) at HH stages 13 to 15 (Figs. 5G,H and data not shown), migrating neural crest cells are in a well-defined mass, with the latest migratory population forming a clear edge at the position of *Brn3a*-positive cells, showing a tight coherence of the two populations. In contrast, in some of the embryos electroporated with a mix of morpholinos against *Wise* and *Wnt6*, the mass of neural crest cells was split or dispersed, without a tight coherence with *Brn3a*-positive cells, when observed in whole mounts (n=6/40) (Fig. 5I,J). Five embryos from the groups of control morpholino, Wise and Wnt6 morpholinos with apparent phenotypes, and Wise and Wnt6 morpholinos without apparent phenotypes, were processed for histological analyses. In control morpholino electroporated embryos, most of delaminated *Brn3a*-positive cells were attached to one or two neural crest cells (Figs. 5K,L). In contrast, in embryos electroporated with Wise and Wnt6 morpholino, the majority of *Brn3a*-positive cells were either not attached to neural crest cells or were attached to one cell (Figs. 5M,N; see Supplementary Fig. 5 for quantification). These results suggest that the expression of *Wise* and *Wnt6* in the surface ectoderm of the trigeminal region might assist the tight assembly of neural crest cells with *Brn3a*-positive placode-derived cells. Electroporation of either *Wise* or *Wnt6* morpholino alone did not show phenotypes as significant as the mixed electroporation when observed in whole mounts (*Wise*, n=7; *Wnt6*, n=9; data not shown).

Electroporation of morpholino oligonucleotides only allowed us to analyze the effect of *Wise* and *Wnt6* at early stages of development, since the electroporated morpholino becomes diluted during the course of rapid growth of the head. In addition, electroporation of morpholino does not attenuate transcription of target genes completely *in vivo* (Supplementary Fig. 4), presumably due to the insufficient electroporation efficiency and insufficient quantity of morpholino introduced in each cell. To verify the endogenous function of Wise in trigeminal ganglion formation, *Wise* was deleted by target-mutation in mice (Supplementary Fig. 6). The *Wise* null mutant was largely normal and viable as previously reported (Kassai et al., 2005), although we found that some null mutants die immediately after the birth, suggesting heterogeneity in the penetration of phenotypes. The mice were analyzed at 10.5 dpc by staining neurofilament to reveal neuronal connections. Wild type embryos showed clear formation of trigeminal ganglia; ophthalmic, maxillary and mandibular branches are distinct at this stage, and the two ganglionic lobes are firmly connected to rhombomere 2 of the hindbrain (Fig. 6A). On the other hand, in *Wise* null mutant mice, although the three branches appear to show the normal projections, the root of the ophthalmic lobe is not attached to the hindbrain, but is either located distally from the hindbrain (Fig. 6B) or is connected poorly by only a few nerves (Fig. 6C). These phenotypes were very mild and found only in 50% of homozygous embryos (n=10), suggesting that the phenotype may well be transient or with low penetration. The phenotype is reminiscent to the one seen in chick when neural crest is removed and the trigeminal ganglion is formed mostly by placode-derived neurons; that is, a delay of afferent projections and separate ophthalmic and maxillomandibular ganglia (Hamburger, 1961; Moody and Heaton, 1983b). On the other hand, the initial migration of neural crest cells, revealed by *sox10* expression at 9.5 dpc, was largely normal in *Wise* homozygous embryos (Figs. 6D–G), suggesting that induction and migrating abilities of neural crest cells are not affected by the loss of Wise expression.

Altogether, these data suggest that Wise expression may induce delamination of the surface ectoderm and promote its coalescence with neural crest cells, leading to the production of ganglionic structures consisting of both origins.

Discussion

The development and differentiation of neural crest cells involves multiple steps, each of which requires accurate and balanced activity of Wnt signaling. Despite the requirement of the Wnt pathway in neural crest development, it has not been clear how Wnt signals are supplied to the migrating neural crest cells. Due to the long distance of migration and reiterative requirement of the signal activation during the course of development, supply of Wnt signals to neural crest cells by other tissues is likely to be required. Focusing on the formation of the trigeminal ganglion, which is achieved by the coalescence of ectodermal and neural crest-derived neurons, we have shown that the Wnt modulator Wise, expressed in the surface

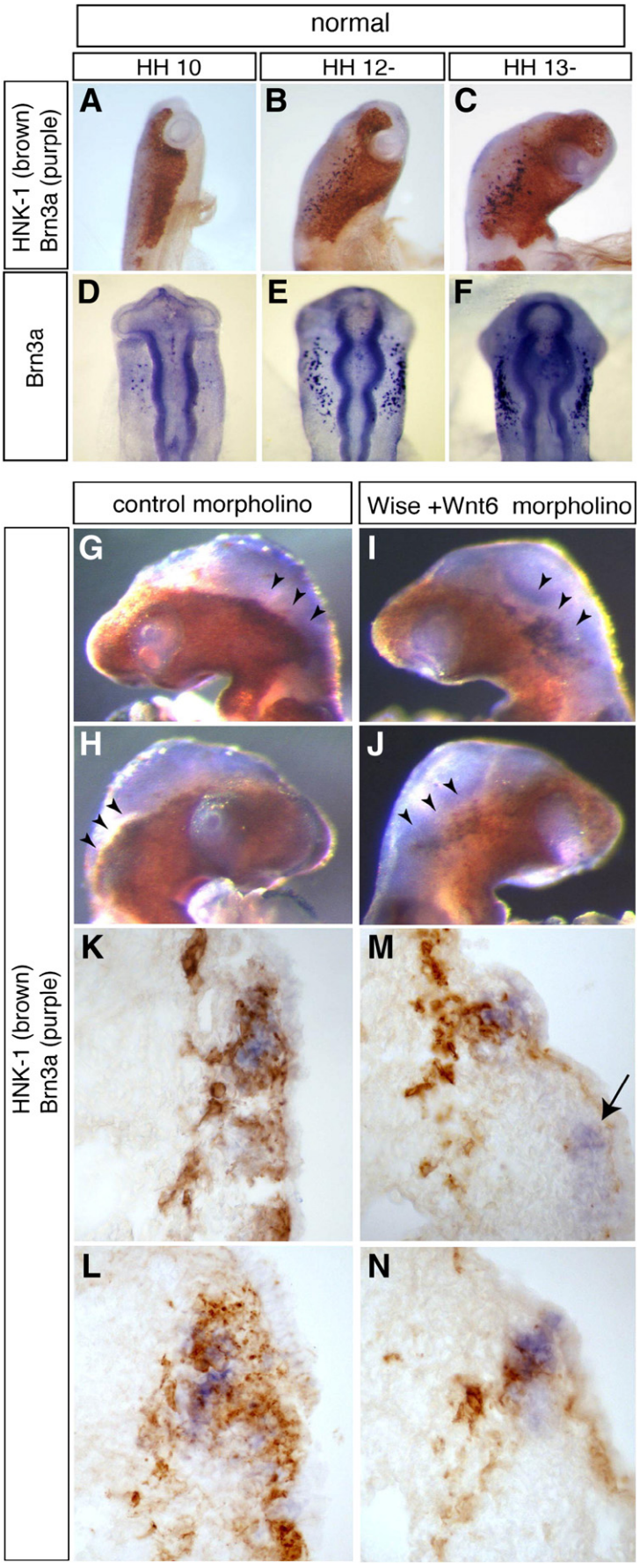
normal
HH 10
HH 12-
HH 13-
HNK-1 (brown)
Brn3a (purple)
A
B
C
Brn3a
D
E
F
control morpholino
Wise +Wnt6 morpholino
HNK-1 (brown)
Brn3a (purple)
G
I
H
J
K
M
L
N

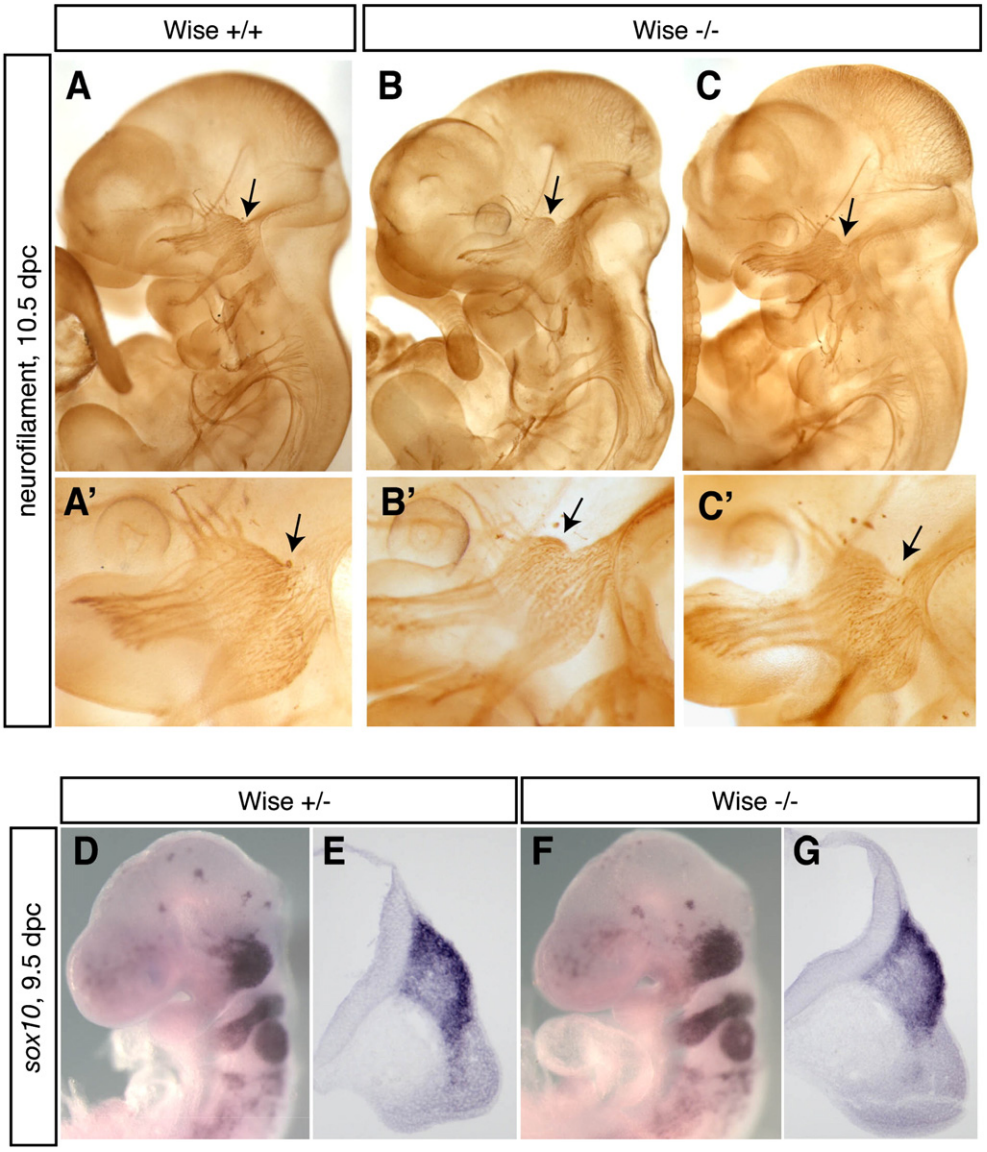

Fig. 6. Wise knockout mice show defects in the connection of the ophthalmic ganglion to the hindbrain. (A–C) Wild type (A) and *Wise* −/− (B,C) littermate embryos at 10.5 dpc stained for neurofilament. Arrows indicate the connection point of the trigeminal ganglion to rhombomere 2. In panel A, the firm connection of the root of the trigeminal ganglion to the hindbrain is seen. In *Wise* −/− embryos, the ophthalmic ganglion is either located distally from the hindbrain with no connection to the hindbrain (B) or is connected only by a few nerves (C). (D–G) *Wise* heterozygous (D,E) and homozygous (F,G) embryos at 9.5 dpc stained for *sox10* by *in situ* hybridization revealing migrating neural crest cells. No significant defects are seen in the homozygous mutant.

ectoderm, is able to function on the migrating neural crest cells. Wise-expressing cells derived from the ectodermal layer appear to attract neural crest cells and promote assembly of the two populations. A possible candidate for the Wnt ligand with which Wise synergizes is Wnt6, as it is expressed in the surface ectoderm in the similar manner to Wise.

Overexpression of Wise causes ectopic trigeminal ganglia

There are a number of possible mechanisms by which over-expressed Wise might induce ectopic ganglia. Wise may have (1) increased induction of neural crest cells; (2) biased the fate of neural crest cells to the trigeminal neurons; (3) promoted placodal cell

Fig. 5. Effect of *Wise* and *Wnt6* morpholinos on migrating neural crest cells. (A–F) Normal embryos stained for *Brn3a* (purple) for trigeminal placodal cells and with HNK1 antibody (brown) for neural crest cells, at stages as indicated on top of the panel. Panels A–C, lateral view; panels D–F, dorsal view. *Brn3a*-positive cells emerge in a speckled manner lateral to the mesencephalon (D), then the position shifts ventro-laterally as the head grows (B,C,E,F). The position of *Brn3a*-positive cells overlaps with the medial edge of the mass of migrating neural crest cells (B,C). (G–N) HH stages 14–15 embryos electroporated with morpholino oligonucleotides against either control (G,H,K,L) or *Wise* and *Wnt6* (I,J,M,N) genes, in the surface ectoderm of the trigeminal region. Embryos were double-stained with markers for neural crest cells (HNK1, brown) and placodal cells (*Brn3a*, purple). While control embryos show the dorsal edge of the mass of neural crest cells overlapping with the *Brn3a*-expressing domain (G,H, arrowheads), *Wise* and *Wnt6*-morpholino electroporated embryos have *Brn3a*-positive cells that do not show a clear overlap with neural crest cells (arrowheads). The dorsal edge of the mass of neural crest cells is not clearly defined, either. Panels K–N show transverse sections across the *Brn3a*-positive trigeminal region of control (K,L) or Wise and Wnt6 (M,N) morpholino electroporated embryos. Dorsal side is to the top. In the control morpholino electroporated embryo (K,L), the *Brn3a*-positive cells (purple) are surrounded by many neural crest cells (brown). In the embryo electroporated with morpholinos against *Wise* and *Wnt6* (M,N), although a comparable amount of *Brn3a*-positive cells are seen, some of them do not show a tight cohesion with neural crest cells. A mass of *Brn3a*-positive cells without any clear adhesion of neural crest cells is indicated by the arrow in panel M. Panels I, J, M are from the group of embryos with apparent phenotypes in the whole mount, while (N) is from the group without apparent phenotypes judged by whole mount observations (See legend of Supplementary Fig. 5). Quantitative analyses of the effects of morpholino oligonucleotides are shown in Supplementary Fig. 5.

differentiation and delamination; (4) promoted the assembly of neural crest cells and placodal cells to form the trigeminal ganglion.

The first possibility, an increase of the neural crest population, is assumed due to the fact that overexpression of Wnt1 or Wnt3a increases the production of neural crest cells in *Xenopus* (Saint-Jeannet et al., 1997), whereas Wnt1 and Wnt3A double knockout mice show a reduction of neural crest cells (Ikeya et al., 1997). As Wise enhances Wnt3a-dependent activation of the Wnt/β-catenin pathway in HEK293 cells (Beaudoin et al., 2005; Guidato and Itasaki, 2007), it is possible that ectopically expressed Wise by virus infection synergizes with Wnt3A to induce neural crest cells. However, Wise overexpression did not cause any significant increase of *Snail2*-positive cells (data not shown), and *Wise* homozygous mutant embryos did not show any significant defect in the production of *sox10*-positive neural crest cells (Figs. 6D–G). In normal embryos, *Wise* is not expressed in the dorsal neural tube or near the region where neural crest cells are produced. Therefore it is unlikely that Wise functions in the production of neural crest cells both in normal and virus-infected embryos.

The second possibility, involvement of Wise in the cell fate determination of neural crest cells, is hypothesized based on the fact that the Wnt/β-catenin pathway is required and sufficient for differentiation of sensory neurons in the anterior head (Hari et al., 2002; Lee et al., 2004). However, surface ectoderm cells delaminated after ectopic *Wise* electroporation did not consistently express Islet-1/2, a neuronal marker (Fig. 4I–L), suggesting that Wise is not involved in determining the neuronal cell fate. In addition, it was noted that while mice with sustained β-catenin expression in the neural crest cell lineage show an increase in sensory neurons and ganglia at the levels of midbrain, hindbrain and spinal cord (Hari et al., 2002; Lee et al., 2004), overexpression of Wise by virus infection induced ectopic ganglia predominantly at the level of midbrain and isthmus. Although the virus infection extended to the posterior hindbrain as well as anterior forebrain, we never found ectopic ganglia posterior to the endogenous mmV or in the post-otic region. Furthermore, although the proximal facial ganglion and ciliary ganglion also contain neurons of both placode and neural crest origin (D'Amico-Martel and Noden, 1983; Lee et al., 2003), ectopic ganglia were not induced in these regions. One possible explanation for this localized effect is that Wnt6, or other possible Wnt ligands, is not expressed in the right place at the right time to induce other ganglia. Another possible mechanism for the ectopic ganglia forming exclusively in the trigeminal region is the unique feature of the ectoderm in the trigeminal region; careful observation of the tissue underneath the surface ectoderm in the ophthalmic region revealed clusters of ganglion-like HNK1-positive neurons, called epidermal nodules (Kuratani and Hirano, 1990). This implies that the ectoderm in the ophthalmic region is susceptible to forming ectopic ganglia, such that the epidermal nodules may act as precursors of and can differentiate into ganglia upon additional promoting factors such as Wnt6 and Wise.

With regard to the third possibility of the function of Wise on the placodal lineage, it is possible that ectopically expressed Wise caused cells to acquire placode-like characteristics, promoting their delamination. This suggestion is based on the observation that ectopic ganglia formed by *Wise* virus infection consisted of not only neural crest cells but also of cells of ectodermal origin (Figs. 2E,F). Interestingly, blocking the Wnt/β-catenin pathway has been shown to block the expression of opV placode markers, and the delamination and neurogenesis of opV placode-derived cells (Lassiter et al., 2007). This supports the idea that ectopic Wise expression promotes the delamination of ectodermal cells in the trigeminal region by enhancing the Wnt pathway. It is however not clear whether ectopic Wise specifically induces trigeminal ganglion-like structures or not. In addition, *Brn3a*, a marker for placode-derived sensory neurons, did not show any specific increase by *Wise* overexpression (Supplementary Fig. 3). Neither *Pax3* nor *Brn3a* are required for the initial formation of the trigeminal ganglion in mice (Eng et al., 2001; Huang et al., 1999; McEvilly et al., 1996; Tremblay et al., 1995), and thus it remains possible that Wise may have promoted the delamination of placodal cells without upregulating either of these genes. It should also be noted that endogenously expressed Wise is unlikely to be involved in the placodal fate decision, because the pre-placodal region is broadly defined before endogenous *Wise* begins to be expressed (Litsiou et al., 2005; Schlosser, 2006). The molecular mechanism of delamination of placodal cells is beginning to be elucidated (Graham et al., 2007), but it is yet to be investigated the mechanism by which Wise induces delamination.

Our result suggested the fourth possibility that Wise-positive delaminated cells attract neural crest cells, which results in promoting the assembly of neural crest cells and placodal cells. This was shown by the tendency of neural crest cells to be attracted to and remain in the Wise-expressing cell aggregates (Fig. 3). The morpholino electroporation experiment supports the possible function of Wise in the assembly of neural crest cells with the delaminated placodal cells (Fig. 5, Supplementary Fig. 5). Altogether, the possible mechanism by which Wise induces ectopic ganglia in overexpression experiments is by increasing delamination of placodal cells and promoting the assembly of neural crest cells with placodal cells.

Wise overexpression also caused changes in the trajectories of trigeminal nerves (Fig. 4). Further studies are required to clarify the mechanism responsible for giving this phenotype. One intriguing issue is that trigeminal sensory neurons detect target (skin)-derived BMP signaling which limit the peripheral innervation in mice (Guha et al., 2004; Hodge et al., 2007). As orthologs of Wise in mouse and rat (Ectodin and USAG-1, respectively) are able to inhibit BMP signaling by binding to BMP (Laurikkala et al., 2003; Yanagita et al., 2004), the phenotype observed in this study might be mediated by the inhibitory function of Wise on BMP signals.

Activation of the Wnt pathway

So far *in vitro* analyses suggest that secreted Wise modulates the activity of the Wnt pathway depending on which ligands are present (Guidato and Itasaki, 2007). Wnt6 is a candidate in the trigeminal region, as it is co-expressed with Wise on the surface ectoderm (Schubert et al., 2002) and Wnt6 overexpression mimics the Wise-overexpression phenotype (Figs. 2B,C). It is however also possible that Wnt1 and Wnt3a, which are expressed in the neural crest before migration, might be other candidates for the partner of Wise. Although the expression of these Wnt ligands are not seen in migrating neural crest cells at the mRNA level, the proteins may remain on the cell surface rather than diffusing away due to their strong association with cell membranes and the extracellular matrix (Reichsman et al., 1996). Hence there remains a possibility that Wise facilitates the activation of the Wnt pathway by these ligands in neural crest cells.

Function of Wise in the trigeminal region

Wise knockout mice have defects in the connection of the ophthalmic ganglion to the hindbrain (Fig. 6). Despite the expression of *Wise* on the surface ectoderm in normal embryos, the phenotype caused by the deletion is reminiscent of defects in neural crest cells. For example, in embryos where neural crest cells are insensitive to Wnt signals due to the selective depletion of β-catenin in neural crest cells, small trigeminal ganglia are formed without connection to the hindbrain (Brault et al., 2001). Ablation of neural crest in chick embryos also causes a similar phenotype (Hamburger, 1961; Moody and Heaton, 1983b; Stark et al., 1997). In addition, Wnt1/3a double knockout embryos show a decrease in neural crest cell formation and a subsequent phenotype of the trigeminal ganglion being positioned

distally with reduced proximal axonal connections (Ikeya et al., 1997), the latter of which is reminiscent of the Wise knockout phenotype. These support the idea that Wise may function cell non-autonomously on neural crest cells.

In contrast to the clear phenotypes by overexpression, the Wise loss of function phenotype in mouse knockout deletion was very mild and subtle (Figs. 6A–C). This could be due to the fact that Wise acts only to facilitate the Wnt pathway, and therefore a loss of Wise is not critical for Wnt pathway activation. The result that *Wise* mutant mice show an incomplete yet structurally clear ophthalmic lobe with correct projections suggests that *Wise* is not required for the development of opV placode-derived neurons.

Acknowledgments

We would like to thank the following people for providing reagents: J. Lindeburg and J. Begbie (chick Brn3a), S.H. Hughes (RCAS), C.L. Cepko (RCAS-ALP), T. Momose (GFP expression vector), and C. Niehrs (mouse Kremen2 signal sequence). We would also like to thank C.V.H. Baker, M. Bronner-Fraser and L. Sommer for critical reading of the manuscript and for suggestions. This work was supported by the Medical Research Council in UK. YS was supported in part by the Japan Society of Promotion of Science and Uehara Memorial Foundation.

Author contributions: YS and NI conceived and designed the experiments. YS performed most of chick *in vivo* experiments and all of *in vitro* ones. The data were analyzed by YS, SG, SH, and NI. Mouse target-deletion was performed by KF and TA, and the subsequent embryo analyses were performed by SH and NI. NI, SH and SG wrote the manuscript with subsequent contributions from all authors.

Appendix A. Supplementary data

Supplementary data associated with this article can be found, in the online version, at doi:10.1016/j.ydbio.2008.04.033.

References

Baker, C.V.H., Bronner-Fraser, M., 2001. Vertebrate cranial placodes I. Embryonic induction. Dev. Biol. 232, 1–61.

Baker, C.V.H., Stark, M.R., Bronner-Fraser, M., 2002. Pax3-expressing trigeminal placode cells can localize to trunk neural crest sites but are committed to a cutaneous sensory neuron fate. Dev. Biol. 249, 219–236.

Beaudoin 3rd, G.M., Sisk, J.M., Coulombe, P.A., Thompson, C.C., 2005. Hairless triggers reactivation of hair growth by promoting Wnt signaling. Proc. Natl. Acad. Sci. U. S. A. 102, 14653–14658.

Begbie, J., Ballivet, M., Graham, A., 2002. Early steps in the production of sensory neurons by the neurogenic placodes. Mol. Cell. Neurosci. 21, 502–511.

Brault, V., Moore, R., Kutsch, S., Ishibashi, M., Rowitch, D.H., McMahon, A.P., Sommer, L., Boussadia, O., Kemler, R., 2001. Inactivation of the beta-catenin gene by Wnt1-Cre-mediated deletion results in dramatic brain malformation and failure of craniofacial development. Development 128, 1253–1264.

Burstyn-Cohen, T., Stanleigh, J., Sela-Donenfeld, D., Kalcheim, C., 2004. Canonical Wnt activity regulates trunk neural crest delamination linking BMP/noggin signaling with G1/S transition. Development 131, 5327–5339.

D'Amico-Martel, A., Noden, D.M., 1983. Contributions of placodal and neural crest cells to avian cranial peripheral ganglia. Am. J. Anat. 166, 445–468.

De Calisto, J., Araya, C., Marchant, L., Riaz, C.F., Mayor, R., 2005. Essential role of non-canonical Wnt signalling in neural crest migration. Development 132, 2587–2597.

Eng, S.R., Gratwick, K., Rhee, J.M., Fedtsova, N., Gan, L., Turner, E.E., 2001. Defects in sensory axon growth precede neuronal death in Brn3a-deficient mice. J. Neurosci. 21, 541–549.

Fedtsova, N., Perris, R., Turner, E.E., 2003. Sonic hedgehog regulates the position of the trigeminal ganglia. Dev. Biol. 261, 456–469.

Fekete, D.M., Cepko, C.L., 1993. Replication-competent retroviral vectors encoding alkaline phosphatase reveal spatial restriction of viral gene expression/transduction in the chick embryo. Mol. Cell. Biol. 13, 2604–2613.

García-Castro, M.I., Marcelle, C., Bronner-Fraser, M., 2002. Ectodermal Wnt function as a neural crest inducer. Science 297, 848–851.

Goulding, M.D., Chalepakis, G., Deutsch, U., Erselius, J.R., Gruss, P., 1991. Pax-3, a novel murine DNA binding protein expressed during early neurogenesis. EMBO J. 10, 1135–1147.

Graham, A., Blentic, A., Duque, S., Begbie, J., 2007. Delamination of cells from neurogenic placodes does not involve an epithelial-to-mesenchymal transition. Development 134, 4141–4145.

Guha, U., Gomes, W.A., Samanta, J., Gupta, M., Rice, F.L., Kessler, J.A., 2004. Target-derived BMP signaling limits sensory neuron number and the extent of peripheral innervation in vivo. Development 131, 1175–1186.

Guidato, S., Itasaki, N., 2007. Wise retains in the endoplasmic reticulum and inhibits Wnt signaling by reducing LRP6 on the cell surface. Dev. Biol. 310, 250–263.

Hamburger, V., 1961. Experimental analysis of the dual origin of the trigeminal ganglion in the chick embryo. J. Exp. Zool. 148, 91–123.

Hamburger, V., Hamilton, H.L., 1951. A series of normal stages in the development of the chick embryo. J. Morphol. 88, 49–92.

Hari, L., Brault, V., Kleber, M., Lee, H.Y., Ille, F., Leimeroth, R., Paratore, C., Suter, U., Kemler, R., Sommer, L., 2002. Lineage-specific requirements of beta-catenin in neural crest development. J. Cell Biol. 159, 867–880.

Hodge, L.K., Klassen, M.P., Han, B.X., Yiu, G., Hurrell, J., Howell, A., Rousseau, G., Lemaigre, F., Tessier-Lavigne, M., Wang, F., 2007. Retrograde BMP signaling regulates trigeminal sensory neuron identities and the formation of precise face maps. Neuron 55, 572–586.

Huang, E.J., Zang, K., Schmidt, A., Saulys, A., Xiang, M., Reichardt, L.F., 1999. POU domain factor Brn-3a controls the differentiation and survival of trigeminal neurons by regulating Trk receptor expression. Development 126, 2869–2882.

Ikeya, M., Lee, S.M., Johnson, J.E., McMahon, A.P., Takada, S., 1997. Wnt signalling required for expansion of neural crest and CNS progenitors. Nature 389, 966–970.

Itasaki, N., Nakamura, H., 1996. A role for gradient en expression in positional specification on the optic tectum. Neuron 16, 55–62.

Itasaki, N., Bel-Vialar, S., Krumlauf, R., 1999. 'Shocking' developments in chick embryology: electroporation and in ovo gene expression. Nat. Cell Biol. 1, E203–207.

Itasaki, N., Jones, C.M., Mercurio, S., Rowe, A., Domingos, P.M., Smith, J.C., Krumlauf, R., 2003. Wise, a context-dependent activator and inhibitor of Wnt signalling. Development 130, 4295–4305.

Kassai, Y., Munne, P., Hotta, Y., Penttila, E., Kavanagh, K., Ohbayashi, N., Takada, S., Thesleff, I., Jernvall, J., Itoh, N., 2005. Regulation of mammalian tooth cusp patterning by ectodin. Science 309, 2067–2070.

Kuratani, S.C., Hirano, S., 1990. The appearance of trigeminal ectopic ganglia within the surface ectoderm in the chick embryo. Arch. Histol. Cytol. 53, 575–583.

Lassiter, R.N., Dude, C.M., Reynolds, S.B., Winters, N.I., Baker, C.V.H., Stark, M.R., 2007. Canonical Wnt signaling is required for ophthalmic trigeminal placode cell fate determination and maintenance. Dev. Biol. 308, 392–406.

Laurikkala, J., Kassai, Y., Pakkasjarvi, L., Thesleff, I., Itoh, N., 2003. Identification of a secreted BMP antagonist, ectodin, integrating BMP, FGF, and SHH signals from the tooth enamel knot. Dev. Biol. 264, 91–105.

Lee, V.M., Sechrist, J.W., Luetolf, S., Bronner-Fraser, M., 2003. Both neural crest and placode contribute to the ciliary ganglion and oculomotor nerve. Dev. Biol. 263, 176–190.

Lee, H.Y., Kleber, M., Hari, L., Brault, V., Suter, U., Taketo, M.M., Kemler, R., Sommer, L., 2004. Instructive role of Wnt/beta-catenin in sensory fate specification in neural crest stem cells. Science 303, 1020–1023.

Lewis, J.L., Bonner, J., Modrell, M., Ragland, J.W., Moon, R.T., Dorsky, R.I., Raible, D.W., 2004. Reiterated Wnt signaling during zebrafish neural crest development. Development 131, 1299–1308.

Litsiou, A., Hanson, S., Streit, A., 2005. A balance of FGF, BMP and WNT signalling positions the future placode territory in the head. Development 132, 4051–4062.

McEvilly, R.J., Erkman, L., Luo, L., Sawchenko, P.E., Ryan, A.F., Rosenfeld, M.G., 1996. Requirement for Brn-3.0 in differentiation and survival of sensory and motor neurons. Nature 384, 574–577.

Momose, T., Tonegawa, A., Takeuchi, J., Ogawa, H., Umesono, K., Yasuda, K., 1999. Efficient targeting of gene expression in chick embryos by microelectroporation. Dev. Growth Differ. 41, 335–344.

Moody, S.A., Heaton, M.B., 1983a. Developmental relationships between trigeminal ganglia and trigeminal motoneurons in chick embryos. I. Ganglion development is necessary for motoneuron migration. J. Comp. Neurol. 213, 327–343.

Moody, S.A., Heaton, M.B., 1983b. Developmental relationships between trigeminal ganglia and trigeminal motoneurons in chick embryos. II. Ganglion axon ingrowth guides motoneuron migration. J. Comp. Neurol. 213, 344–349.

Murata, T., Furushima, K., Hirano, M., Kiyonari, H., Nakamura, M., Suda, Y., Aizawa, S., 2004. ang is a novel gene expressed in early neuroectoderm, but its null mutant exhibits no obvious phenotype. Gene Expr. Patterns 5, 171–178.

Ogasawara, M., Shigetani, Y., Hirano, S., Satoh, N., Kuratani, S., 2000. Pax1/Pax9-Related genes in an agnathan vertebrate, *Lampetra japonica*: expression pattern of LjPax9 implies sequential evolutionary events toward the gnathostome body plan. Dev. Biol. 223, 399–410.

Petropoulos, C.J., Hughes, S.H., 1991. Replication-competent retrovirus vectors for the transfer and expression of gene cassettes in avian cells. J. Virol. 65, 3728–3737.

Reichsman, F., Smith, L., Cumberledge, S., 1996. Glycosaminoglycans can modulate extracellular localization of the wingless protein and promote signal transduction. J. Cell Biol. 135, 819–827.

Saint-Jeannet, J.P., He, X., Varmus, H.E., Dawid, I.B., 1997. Regulation of dorsal fate in the neuraxis by Wnt-1 and Wnt-3a. Proc. Natl. Acad. Sci. U. S. A. 94, 13713–13718.

Schlosser, G., 2006. Induction and specification of cranial placodes. Dev. Biol. 294, 303–351.

Schubert, F.R., Mootoosamy, R.C., Walters, E.H., Graham, A., Tumiotto, L., Munsterberg, A. E., Lumsden, A., Dietrich, S., 2002. Wnt6 marks sites of epithelial transformations in the chick embryo. Mech. Dev. 114, 143–148.

Shigetani, Y., Itasaki, N., 2007. Expression of Wise in chick embryos. Dev. Dyn. 236, 2277–2284.
Stark, M.R., Sechrist, J., Bronner-Fraser, M., Marcelle, C., 1997. Neural tube-ectoderm interactions are required for trigeminal placode formation. Development 124, 4287–4295.
Tahinci, E., Thorne, C.A., Franklin, J.L., Salic, A., Christian, K.M., Lee, L.A., Coffey, R.J., Lee, E., 2007. Lrp6 is required for convergent extension during *Xenopus* gastrulation. Development 134, 4095–4106.
Taneyhill, L.A., Bronner-Fraser, M., 2005. Dynamic alterations in gene expression after Wnt-mediated induction of avian neural crest. Mol. Biol. Cell 16, 5283–5293.
Tremblay, P., Kessel, M., Gruss, P., 1995. A transgenic neuroanatomical marker identifies cranial neural crest deficiencies associated with the Pax3 mutant Splotch. Dev. Biol. 171, 317–329.
Wurst, W., Auerbach, A.B., Joyner, A.L., 1994. Multiple developmental defects in Engrailed-1 mutant mice: an early mid-hindbrain deletion and patterning defects in forelimbs and sternum. Development 120, 2065–2075.
Yagi, T., Tokunaga, T., Furuta, Y., Nada, S., Yoshida, M., Tsukada, T., Saga, Y., Takeda, N., Ikawa, Y., Aizawa, S., 1993. A novel ES cell line, TT2, with high germline-differentiating potency. Anal. Biochem. 214, 70–76.
Yanagita, M., Oka, M., Watabe, T., Iguchi, H., Niida, A., Takahashi, S., Akiyama, T., Miyazono, K., Yanagisawa, M., Sakurai, T., 2004. USAG-1: a bone morphogenetic protein antagonist abundantly expressed in the kidney. Biochem. Biophys. Res. Commun. 316, 490–500.